# Reinforced Concrete Beams Enhancing Flexural Capacity Via Hybrid FRP Strengthening: Experimental Numerical Investigation

Asjad Javed[1], Dr. M. Adil Khan[2], Abdul Rehman Ghumman[3], Waqas Aziz[4], Engr. Baitullah Khan Kibzai[5], Kashif Daud[6], Abdul Haq[7*], Samiullah Memon[8]

[1.] Communication and Works Department, Punjab, Pakistan
[2.] Resident Engineer (RE), National Engineering Services Pakistan (NESPAK), Lahore, Pakistan
[3.] Communication and Department, Pakistan
[4.] University of Southern Punjab Multan, Pakistan
[5.] Senior Engineer, PCSIR, Karachi, Pakistan
[6.] Khyber Pakhtunkhwa Urban Mobility Authority, Transport & Mass Transit Department, Khyber Pakhtunkhwa, Pakistan
[7.] School of Civil Engineering Southeast university, 211189, Nanjing, China, Advance Ocean Institute of Southeast University Nantong, China
[8.] Mehran University of Engineering and Technology, Jamshoro, Sindh, Pakistan
*Corresponding Author: Abdul Haq

**Abstract**
Structural reviews and inspections can identify weaknesses in existing buildings, especially in older structures that may necessitate appropriate retrofitting or restoration. More, FRP composites are widely utilized owing to their superior reinforcing capabilities in restoration projects. This study investigates the use of hybrid FRP (HFRP), aramid FRP (AFRP), and glass FRP (GFRP) laminates and sheets to enhance the flexural performance of reinforced concrete (RC) beams through a combination of experimental & numerical investigations. Five RC beams with a reinforcement ratio of 0.47% were cast and tested under four-point bending, with one beam serving as the control specimen and the remaining four strengthened using HFRP laminates of different thicknesses. The results show that HFRP strengthening substantially enhances the load-carrying capacity; however, increasing laminate thickness beyond an optimum level is not recommended. Epoxy bonding and concrete surface condition substantially affect flexural performance. The beam strengthened with HFRP3 (SH3) exhibited an ultimate load increase of 202.63%. Finite element analysis was also conducted, and the numerical results demonstrated close agreement with the experimental findings, confirming the reliability of the modeling approach.
**Keywords:** Flexural strength, RC beams, Composite materials, HFRP, Flexural strength

## 1. INTRODUCTION

Fiber-reinforced polymer composites gained prominence as structural strengtheners in the 1980s (Diniţ,ă et al., 2024). Routine strengthening of reinforced concrete structural components is performed to modify loads, preserve structural integrity, and reduce aging- related damage (Duvnjak et al., 2021). External FRP systems have been shown to enhance and restore deficient structural components (Sharba et al., 2021). Fiber-reinforced plastic (FRP) materials exhibit superior stiffness, lightweight properties, strength-to-weight ratios, corrosion

resistance, flexibility, ease of installation, and diversity compared to steel and aluminum plates (Mahboubizadeh et al., 2024). Fiber-reinforced plastic (FRP) enhances concrete (RC) flexural & beams shear capacity at room temperature more effectively than textile mortar (Ghanem et al., 2023). GFRP, CFRP, and AFRP laminates are commonly employed for structural reinforcement (Smarzewski et al., 2022a). Strengthening methods are designed to enhance structure's flexural strength, and longevity under various loading conditions. Reinforcement of structures enhances both performance and longevity. Hence, FRP composites are utilized in study for the reinforcement and repair of structures. Near-surface-mounted & external-bonded strengthening methods more effective. Reinforcement of RC beam soffits can be achieved using FRP sheets bonded with a resin matrix (Panahi et al., 2021). However, Laminates frequently hired for enhancing structural strength of beams. The technique, in which laminates are folded around a beam, effective method for reinforcing fiber-reinforced plastic beams. Structural support, however, inhibits the implementation of this strategy. Utilizing U-shaped FRP laminates to wrap the beam is a prevalent and effective approach; however, the cost of de-bonding is high. The application of bonded outer reinforcement on the sidewalls of the reinforced concrete beam does not enhance its load capacity. Laminates are employed to cover the soffit of recycled concrete beams, a practice that is both uncommon and cost-effective. Numerous studies indicate that the interfacial bond association between FRP laminate & reinforced concrete significantly influences FRP-reinforced concrete structures. Modification processes are employed because FRP reinforced concrete beams and slabs exhibit a loss of ductility. The inclusion of fiber in composite materials is restricted; however, the blending of conventional materials can mitigate this limitation. This enhances the mechanical properties of composites. The integration of composite and conventional materials can enhance mechanical properties. Hybrid materials integrate the strengths of one material to address the weaknesses of another. In recent years, the popularity of HFRP has increased. FRP sheets of various thicknesses, strengths, ductility, and stiffnesses are used to assemble the composites. The composites include aramid/Kevlar, carbon, and glass. AFRP exhibits superior chemical resistance, longitudinal tensile strengths, high-tensile modulus, and lower production costs when compared to carbon fibre reinforced plastic (CFRP). AFRP is appropriate for hybrid composite applications. Glass- Kevlar mixture improves compressive strength, fiber-matrix connection at the interface, flexural modulus, and thermal characteristics (Chinnasamy et al., 2020). Kevlar fiber enhances the flexural properties of composites. Glass fiber reinforced plastic (GFRP) is significantly less expensive than carbon fiber reinforced plastic. The materials show improved deformability, energy absorption, impact resistance, and lower tensile modulus and strength (Panahi et al., 2021). GFRP exhibits superior thermal properties, cost-effectiveness, and robust heat resistance. Aramid fibres exhibit significant differences in compressive and tensile strengths. A mix of GFRP and AFRP can solve various problems. Reinforced concrete beams that had been broken and punctured were covered with AFRP sheets. The research determined how much weight the strengthened beams could bear (Said et al., 2022).

In the 1980s, FRP composites became popular structural strengtheners (Abbood et al., 2021). RC structural components are regularly strengthened to change loads, maintain structure integrity, and minimise aging-related structural deterioration (Rincon et al., 2024). FRP exteriors strengthen and repair structural elements. FRP materials beat steel and aluminum plates in rigidity, weight, and diversity. At ambient temperature, FRP outperforms textile-reinforced mortar in increasing RC beams capacities. Reinforcements can be created by using GFRP, CFRP, or AFRP laminates (Smarzewski et al., 2022b). The shear and flexural strengths,

as well as the ductility and durability of a structure, can be enhanced through strengthening. Structures perform better and last longer when reinforced. Research has reinforced and repaired structures with FRP composites. NSM and external-bonded strengthening work. RC beam soffits can be reinforced with FRP sheets and resin matrix (Derkowski & Walczak, 2021). Beams are often strengthened with laminates. One of the best ways to reinforce fiber-reinforced plastic beams is to fully cover them in laminates. Although structural support precludes this technique from being applied. U-shaping the beam with FRP laminates is common and efficient, but de-bonding is expensive. Bonded outer reinforcement on RC beam sides does not increase load capacity. Rare and cheaper laminates cover the recycled concrete beams' soffit. Several studies revealed FRP laminate-RC interfacial bond greatly impacts FRP reinforced RC structures. Because concrete beams and slabs reinforced with FRP tend to show limited ductile behavior, design & detailing modifications are implemented for enhanc performance. Composite materials have limited fibre integration, but combining conventional materials can prevent this. This enhances composite mechanical properties. Combining composite and traditional materials improves mechanical properties. Hybrid materials combine the strengths of two materials. In recent years, HFRP has gained popularity. Composites are assembled using FRP sheets of varied thicknesses, strengths, ductility, and stiffness. Carbon, glass, and aramid/Kevlar composites. AFRP provides better chemical resistance, longitudinal tensile strengths, high tensile modulus, less elongation after breakage, and reduced production costs than CFRP. AFRP works for hybrid composites. Glass-kevlar hybrids improve compressive strength, fiber-matrix bonding at the interface, flexural modulus, and thermal characteristics. Fibre Kevlar enhances composite flexural properties. Glass fibre reinforced plastic (GFRP) is cheaper than CFRP. They have better deformability, energy absorption, impact resistance, and reduced tensile modulus and strength. GFRP is inexpensive, heat-resistant, and thermally efficient (Derkowski & Walczak, 2021). Compressive and tensile strengths vary greatly in aramid fibers. A GFRP-AFRP blend can solve several issues. Pre-cracked, apertured RC beams bonded to AFRP. Osman and colleagues tested the massive load capacity.

## 2. PROCEDURE FOR MATERIALS

### 2.1. Materials

#### 2.1.1. The Concrete-Mix

Following a curing period of 28 days, cubes with expected compressive strength produced with concrete mix, as per the proportions outlined in IS 10262:2019 and IS 456:2000, is 38 MPa. Ready-mix concrete is employed to ensure that all batches are produced in alignment with the mix design established through laboratory material testing. The concrete of M30 grade is characterized by a 1.002 MPa standard deviation and 0.030 coefficient of variance. Following the casting process, the beams are subjected to a water curing procedure that extends over a duration of 28 days. Additional samples, such as prisms, cubes, and cylinders, are cast and evaluated to ascertain material strength properties. After curing 28 days, concrete cubes' prisms' and cylinders' split strength averaged 36 MPa, 4.77 MPa, and 40 MPa. Concrete would be made with Table 1's ingredients.

**Table 1 M30 concrete Materials utilized (cubic meter)**

| Water | Water/Cement Ratio | Cement | Coarse aggregate | Fine Aggregate | Superplasticizers |
|---|---|---|---|---|---|
| 1.44 | 0.44 | 360 | 1196 | 752 | 3.6 |

**Table 2 Steel Bars Material Attributes.**

| Strength Yield (MPa) | Diameter | Strength Tensile (MPa) |
|---|---|---|
| 343 | 8 | (473) |
| 362 | 10 | (566) |

### 2.1.2. Steel Reinforcement Bar

Fe500 grade is used in the production of the reinforcing bars that have a high yield strength. For the purpose of evaluating rebar stress-strain properties, eight- & ten-millimetre diameter coupons are manufactured and then subjected to tensile loading. The results that were obtained are presented in Table 2 below.

### 2.1.3. HFP laminates.

The study uses unidirectional E-glass and aramid fibres. Hand-laid HFRP laminates are made. Hardener and epoxy resin are mixed 1:10 to bond ply sheets into laminates. Reinforcing reinforced concrete beams with externally bonded FRP uses 3000 mm by 150 mm unidirectional high-strength laminates. American Society of Testing & Materials (ASTM) standard tensile and flexural tests were used to measure the four HFRP coupon specimens' mechanical properties. Table 3 lists HFRP laminate mechanical properties. Figure 1 shows HFRP laminates used to reinforce concrete beams.

**Table 3 HFRP laminates Properties**

| Laminate Type | Flexural Strength (MPa) | Flexural Modulus (GPa) | Thickness (mm) | Tensile Strength (MPa) | Tensile Modulus (GPa) |
|---|---|---|---|---|---|
| HFRP1 | 208 | 7.98 | 3.4 | 212 | 10.25 |
| HFRP2 | 221 | 8.36 | 4.5 | 234 | 11.92 |
| HFRP3 | 254 | 9.55 | 5.6 | 267 | 12.67 |
| HFRP4 | 291 | 9.96 | 6.3 | 302 | 14.26 |

### 2.1.4 Epoxy Resin Matrix

A resin and a hardener that is composed of epoxy are utilized in order to guarantee that the laminates produced from high-fiber reinforced plastic (HFRP) will adhere properly to the surface of the concrete. A ratio of one resin to one-half of a hardener is used. The following concrete impregnators are utilized by the researcher: COROCRETIN IHL 18 - COMP B, COROCRETIN IHL 18 - COMP A, and COROCRETIN FILLER SL. It is responsibility of the manufacturer to give the material properties. Table 4 provides a breakdown of the properties of the resin and hardener that were selected.

**Table 4 Resin Properties**

| | **Consequence** |
|---|---|
| Type | Two-pack cold-cure |
| Density(g/cc) | 1.10–1.20 |
| Mix-ratio(Component A: B) | 2:1 |
| Flexural-strength | 45 |
| Tensile-strength | 23 |
| Shear-strength | 22 |
| Composition | Epoxy resin with formulated hardener |
| Compressive-strength | 100 |

**Figure 1 HFRP laminates.**

## 2.2 Test procedure

### 2.2.1 RC Beam Specs

The experimental program examined the flexural behaviour of five simply supported reinforced concrete (RC) beam specimens (Figure 2). All beams were cast with identical geometric and reinforcing details, 3000 mm long, 2800 mm effective span, 150 mm cross-sectional width, and 250 mm depth. Even, 10 mm steel bars in tension & compression zones supplied longitudinal reinforcement, while 8 mm closed-loop steel stirrups spaced 150 mm along the beam length provided shear reinforcement. The beams were intentionally under-reinforced according to IS 456:2000's limit state design technique (Abbood et al., 2021). As shown in Table 5, the experiment compared RC beam flexural strength. Longitudinal reinforcement ratio was longitudinal steel reinforcement ratio to beam section. Four of the five specimens were externally strengthened with HFRP composite laminates, while one was left as a control specimen for comparison.

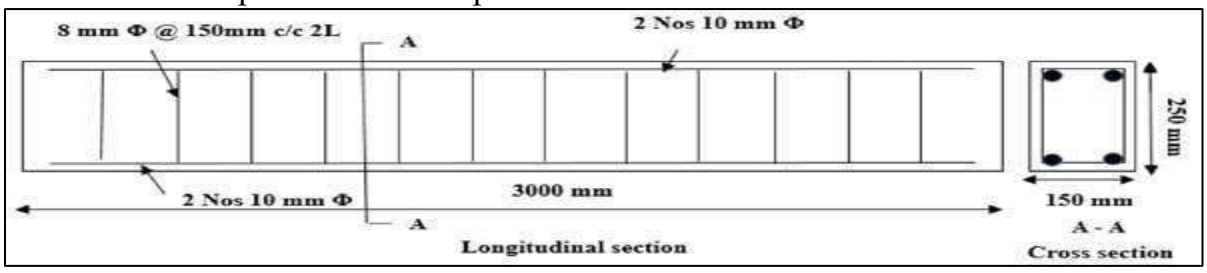


**Figure 2: steel reinforcing details & Beam geometry - steel reinforced bars Diameter.**

**Table 5 RC-Beam Specimens Detail**

| Designation of Beam | FRP-Strengthened Beam Type | Fibers Combination (%) |
|---|---|---|
| SH(5) | – | – |
| SH(1) | HFRP(1) | 90% Glass(G)/10% Aramid(A) |
| SH(2) | HFRP(2) | 80% Glass(G)/20% Aramid(A) |
| SH(3) | HFRP(3) | 70% Glass(G)/30% Aramid(A) |
| SH(4) | HFRP(4) | 60% Glass(G)/40% Aramid(A) |

### 2.2.2. Casting and Curing

In the present experimental program, five reinforced concrete (RC) beams were cast and tested, all featuring a longitudinal reinforcement ratio of 0.47%. One beam was left unstrengthened to serve as the control specimen, while the other four were strengthened at the soffit using four distinct types of HFRP laminates. Each beam was reinforced with two 10-mm-diameter steel bars in both the tension and compression zones. Wooden molds were used for casting, and the reinforcement cages were fabricated and secured with tie wires to ensure proper alignment and spacing. Prior to mounting electrical resistance strain gauges (120 Ω resistance, gauge factor of 2), a 10-mm segment of the tension reinforcement bar at mid-span was ground and polished with fine sandpaper to ensure proper adhesion. All specimens were cast in a single batch using the gang casting method. The internal surfaces of the molds were oiled before concreting to facilitate easy demolding. Layers of concrete were crushed via needle vibrator to reduce voids. Demolded soon after 24 hours, the beams were water-cured. Therefore, casting & curing procedures are illustrated schematically in Figure 3.

**Fig. 3.** Casting and curing of beam the specimens.

### 2.2.3. RC beams Procedure Strengthening

After 28 days of cure, RC beams are externally strengthened. ACI 440.2R bonds hybrid fiber-reinforced polymer (HFRP) sheets to beam soffits to strengthen bending. The concrete surface is first abraded to remove the weak laitance layer, followed by grinding to create a clean, uniform, and sound bonding surface. A uniform layer of epoxy adhesive is then applied to ensure consistent impregnation and optimal adhesion. HFRP, fabricated via the hand lay-up method, is cut to the required dimensions & carefully positioned onto an adhesive-coated surface. A roller is used to press the laminate firmly, expelling trapped air and ensuring full contact with the concrete. To improve bond quality and consolidation, dead loads are positioned on the laminate during curing, & the strengthened beams left undisturbed for 4 to

6 days before testing. The complete sequence of this strengthening procedure is depicted in Figure 4.


**Figure 4. Diverse-shaped RC Beams**

### 2.2.4 Test setup:

The specimens, illustrated in (Fig. 5a), were simply supported with approximate bearing lengths of 100 mm at each end and an effective span of 2800 mm. The reinforced concrete (RC) beams underwent 4-point bending tests using a loading frame. Hence, a load was delivered through a hydraulic actuator capable of a maximum load of 400 kN, and beams flexural response was recorded throughout the experiment. A stepwise loading procedure was followed, increasing the load in increments of 5 kN until beam failure. Beam deflections were measured using 3 dial gauges: first positioned at mid-span and second beneath loading points. Dial gauges 0.01mm least count captured deflections at each increment. Strain measurements were collected manually through strain gauges linked to four-channel strain indicators. Even the applied load from the load cell was transmitted to the beam using a longitudinal stiff steel beam. The beams were supported at the ends with a combination of a hinge and roller to allow rotation. The complete instrumentation layout for the tested beams is presented in Fig. 5b.

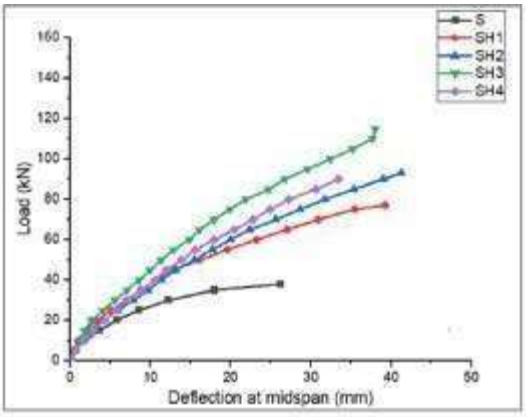


**Fig. 6.** The deflection due to load applied on RC beams.

## 3. RESULTS AND DISCUSSION

This is a response of the RC beam under loading and displacement. The S mentions control beam reached a final load of 38 kN when 26.33 mm mid-span deflection. Of tested specimens, reinforced-beam SH3 had highest load carrying capacity amounting to 115 kN, which is 202.63 % higher. At failure, SH3 achieved 38.03mm mid-span deflection. However, the strengthened beams had higher ultimate strength than the unstrengthened beam, as do the strengthened beams, and this indicates the strengthening led to an increase in ductile behavior. Hence, evaluation of the reinforced beams compares and contrasts the load-bearing capacity with the increase in the sheet thickness of the sheets of HFRP up to a thickness of 5.6 mm. The beam reinforced with four HFRP sheets (SH4) however, began to debond the laminate at the concrete surface prematurely, which means that the ultimate load was less than expected; 90 kN even though it was thicker. Such an observation is an indication that bond performance can be negatively affected by too much laminate thickness. All RC beams load-deflection responses are shown in Fig. 6. The results also show that a significant rise in the FRP thickness of about 50 percent resulted in a relatively slight increase in 20 % load-carrying capacity, as is evident between beams SH3 and SH4. These results imply that the flexural capacity of HFRP laminate is maximized at certain point of increased laminate thickness, and thereafter, the strengthening effectiveness decreases. The trend noticed can be compared to the results given by Ortiz et al. (2023).

### 3.1 Beam failure Mode

All five beam specimens first started vertical cracking in the tension face at a load of 20 to 35 kN and propagated to the compression zone located within the moment region, and with additional loading, flexural cracks were formed randomly in the constant moment zone and all the specimens were quite ductile before the flexural cracking. In the enhanced beams, the cracks on the tension side that occurred controlled the failure, and the existence of laminates prevented widening of the cracks which was substantially narrower than the cracks present on the control beam during loading process; as the load increased, more cracks also developed within the shear span. The control specimen (S) failed mostly in flexure, whilst specimen SH1 experienced flexural cracking and epoxy debonding. Specimen SH2 failed because of debonding through a flexural-shear crack, whereas specimen SH3 failed with flexural cracking and epoxy debonding in shear span, which agrees with crack patterns by Lin et al. (2021). In

the case of sample SH4, failure was determined as debonding in the form of flexural-shear crack, which developed in the area between the loading point and the support area.

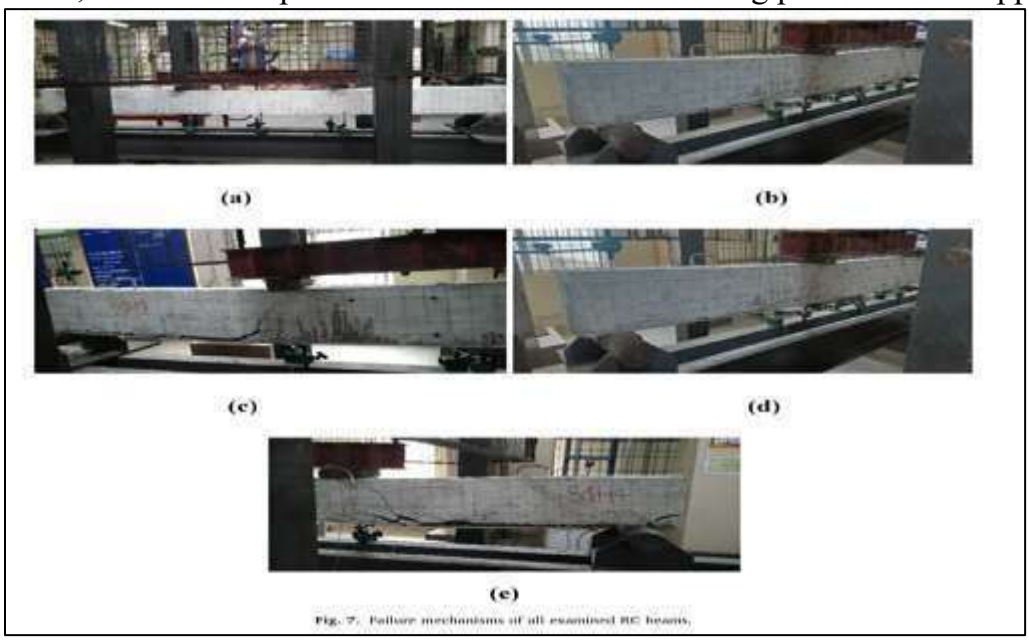


Fig. 7. Failure mechanisms of all examined RC beams.

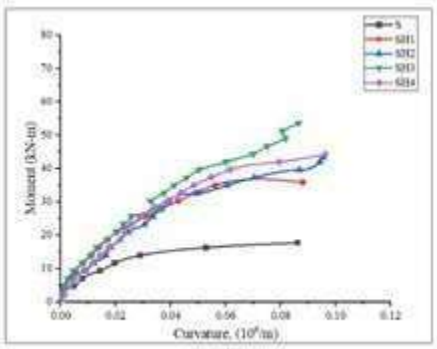


Fig. 8. Moment – curvature behavior of RC beams.

### 3.3. Moment-curvature behavior

Figure 8 presents the results of moment-curvature of tested RC beams using experimental program. The moment-capacity (M) that shows the resistance of the beam to rotational deformation caused by flexural loads was determined by applying equation (1):

$$M = 0.5 \times P \times a \quad (1)$$

Where P, shear span is represented by a. The evaluation of curvature, which shows the deformation of the beam after loading that is manifested as bending, was measured by dial gauges displacements in compression and tension zones. Those displacement measurements then were converted to strain values to measure the curvature. The findings show that HFRP strengthening has a strong ability to improve the curvature at failure, and flexural ductility is improved. Besides, the hybrid-strengthened beams showed similar patterns in moment-curvature, as it is reported by Qi et al. (2023).

### 3.4. Energy Absorption and Stiffness at Cracking: Comparison.

The energy absorption capacity of the beams was evaluated by calculating the area under the load–deflection curve, while the cracking stiffness was determined as the ratio of the first crack load to its corresponding deflection, serving as a key indicator of how effectively the strengthening technique improved the beam's elastic response and rigidity. Results revealed

that HFRP-strengthened beams absorbed nearly twice the energy of the unstrengthened control beam, demonstrating a significant boost in structural performance. All strengthened specimens showed markedly higher energy absorption and cracking stiffness compared to the control, with a comprehensive summary of these findings provided in Table 6.

**4Numerical simulation**

The ABAQUS finite element analysis (FEA) software was implemented in numerical simulations, and it can handle both geometric and material nonlinearities of three-dimensional problems. The experiment program geometry and dimensions were the same as those of all the components in the numerical model. The modeling process used in this research project is the finite element modeling and was explained in depth in the sections below.

**Table 6 Parameters Properties**

| | SH3 | SH4 | SH2 | SH1 | SH5 |
|---|---|---|---|---|---|
| Ultimate load | 115 | 90 | 93 | 77 | 38 |
| Ultimate-moment (kN·m) | 53.65 | 41.99 | 43.38 | 35.92 | 17.72 |
| Ultimate-deflection (mm) | 38.03 | 33.44 | 41.27 | 39.24 | 26.23 |
| Deflection at yield load (mm) | 26.8 | 24.0 | 29.7 | 23.8 | 14.2 |
| Yield load(kN) | 92 | 72 | 74 | 62 | 30 |
| Ductility ratio | 1.42 | 1.47 | 1.44 | 1.69 | 2.15 |
| Cracking Stiffness (kN/mm) | 5.40 | 4.38 | 4.22 | 4.00 | 2.93 |
| Rebar strain load (μm/m) | 1567 | 1391 | 1745 | 2325 | 2710 |
| Energy absorption capacity (kN·mm) | 2565.53 | 2493.63 | 2354.23 | 2019.08 | 722.3 |

### 4.1. Concrete

Three-dimensional eight-node C3D8R elements with decreased integration model the bream concrete portion. The Concrete Damaged Plasticity model simulates tensile cracking and compressive crushing as key failure modes. This model represents concrete's inelastic response using isotropic damaged elasticity and plasticity in tension and compression. It defines strain in compression and compensates strain rate sensitivity, simulating concrete behavior realistically as described by Siamakani et al. 2022 and Shaheen et al. 2023. Figure 9 a-b illustrates concrete's tensile characteristics & compressive stress–strain curve, and Table 7 lists the model's input values.

**Table 7: Concrete Model Parameter**

| Parameters | Value |
|---|---|
| Ratio of biaxial to uniaxial compressive strength, σb0/σc0 | 1.16 |
| Flow potential eccentricity, ε | 0.10 |
| Viscosity parameter, μ | 0 |
| Second stress ratio | 0.667 |
| Dilation angle, Ψ | 31 |

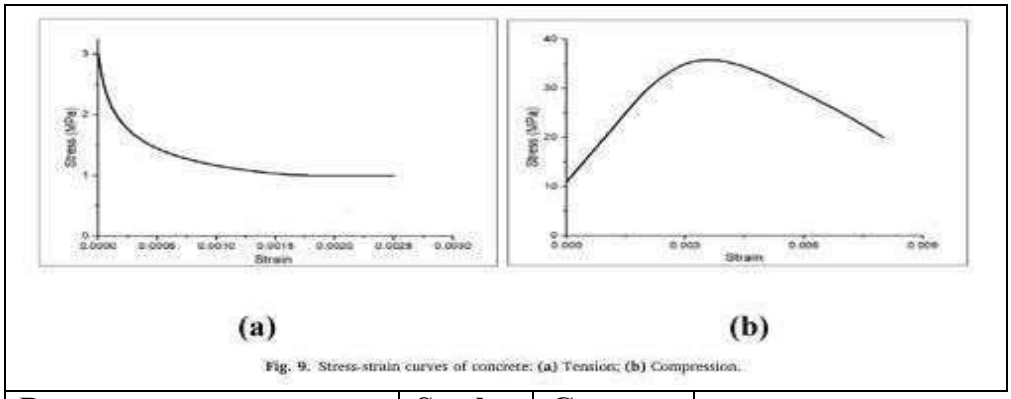


Fig. 9. Stress-strain curves of concrete: (a) Tension; (b) Compression.

| Parameters | Steel | Concrete |
|---|---|---|
| Young's modulus, *E* (MPa) | 214,780 | 30,033 |
| Poisson's ratio, *v* | 0.30 | 0.18 |

### 4.2. Steel

The reinforcing steel bars were simulated via elastic perfectly plastic material model, with isotropic strain hardening applied to all bar diameters. The outcomes of the experimental tests are presented in Table 8. In the finite element analysis, steel reinforcement was modeled as three-dimensional truss elements (T3D2), while bonds between reinforcement and surrounding concrete were captured through an embedded region constraint.

**Table 8**: **Concrete Parameters & steel-model**

| | Steel | Concrete |
|---|---|---|
| Young's modulus, E (MPa) | 214,780 | 30,033 |
| Poisson's ratio, *v* | 0.30 | 0.18 |

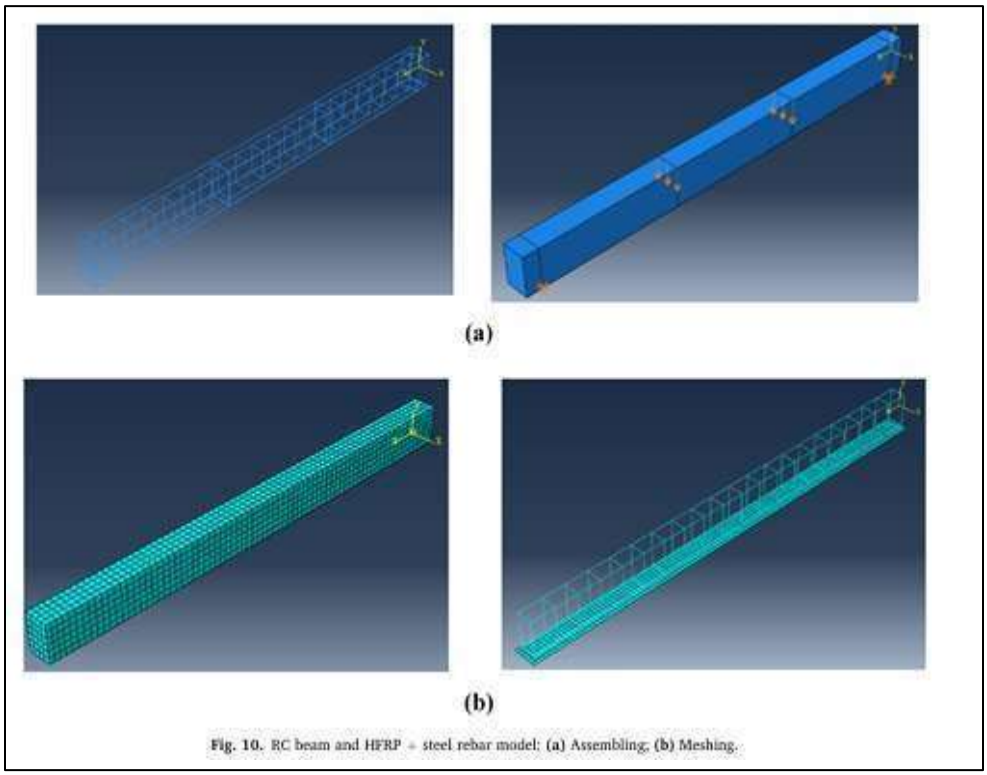


Fig. 10. RC beam and HFRP + steel rebar model: (a) Assembling; (b) Meshing.

### 4.3. HFRP laminates

S4R elements were used to model HFRP laminates, which were assumed to be elastic up to brittle failure at maximum tensile stress. The lamina material model reflected isotropic elastic behavior, with longitudinal and transverse moduli. Four-node conventional shell elements demonstrate HFRP (S4R) sheets' behavior. FRP sheets are elastic until brittle failure at maximum tensile stress. The lamina material mimics HFRP sheets' isotropic behavior. Ex, Ey Poisson's ratio, Gxy, Gxz shear modulus in xy , xz, and yz planes, and Gyz are 4.4. Table 9 summarizes it, and the tie constraint simulated a perfect HFRP-concrete connection. Concrete, stirrups, longitudinal tension and compression reinforcement, and HFRP laminates were used to build the RC beams using the Part module. All material properties and element assignments were defined in Property and assembled in Assembly. The concrete-HFRP interface was modeled using tie constraint and the concrete-steel reinforcement interaction was modeled using embedded region constraint. In Fig. 10a, fixed translational and rotationally free supports and vertical loading on the top surface were boundary conditions. The model's meshing optimization, which used 40-50 mm mesh size depending on mesh sensitivity study, was crucial. Each part's mesh size was allotted to ensure accuracy and computing efficiency. FE jobs were generated and performed by the Job module, evaluated and visualized through the Visualization module, and mesh set up and boundary conditions shown in Fig. 10b.

**Table 9: HFRP sheets Properties**

| FRP Type | *G*xy = *G*xz (GPa) | *G*yz (GPa) | *E*x (GPa) | *E*y (GPa) | *ν*xy |
|---|---|---|---|---|---|
| HFRP1 | 2.63 | 2.34 | 32.68 | 6.79 | 0.29 |
| HFRP2 | 2.57 | 2.29 | 35.64 | 6.64 | 0.29 |
| HFRP3 | 2.53 | 2.24 | 38.11 | 6.52 | 0.29 |
| HFRP4 | 2.43 | 2.18 | 42.01 | 6.32 | 0.30 |

### 4.5. Numerical Modelling Validation

Experimental load and deflection results and FEA models utilized for evaluation and model verification. The predicted and determined load against deflection curves at all loading stages are displayed in Fig. 11. Results show that the numerical models and experiments agree. The numerically modeled specimens' displacement and stresses are shown in Fig. 12. The observed failure modes match the experimental results. Table 10 compares experimental and FEA results. The study uses Pu to represent the ultimate load and δu to represent the mid-span deflection of the RC beams. The permissible deflection limit in IS 456:2000 is Δ per. Table 11 compares serviceability deflection limitations. IS 456:2000 allows deflection. The experimental and FEA ultimate loads and deflections differed by less than 13%. Many cracks appeared after flexural cracks appeared in the specimens. FE model strengthened beams showed deboned cover concrete when it failed. As shown in Fig. 13, the FE models accurately captured beam failure modes, including initial cracking and eventual failure with/without FRP reinforcement. Shear cracks and flexure are more prevalent in RC beam SH4.

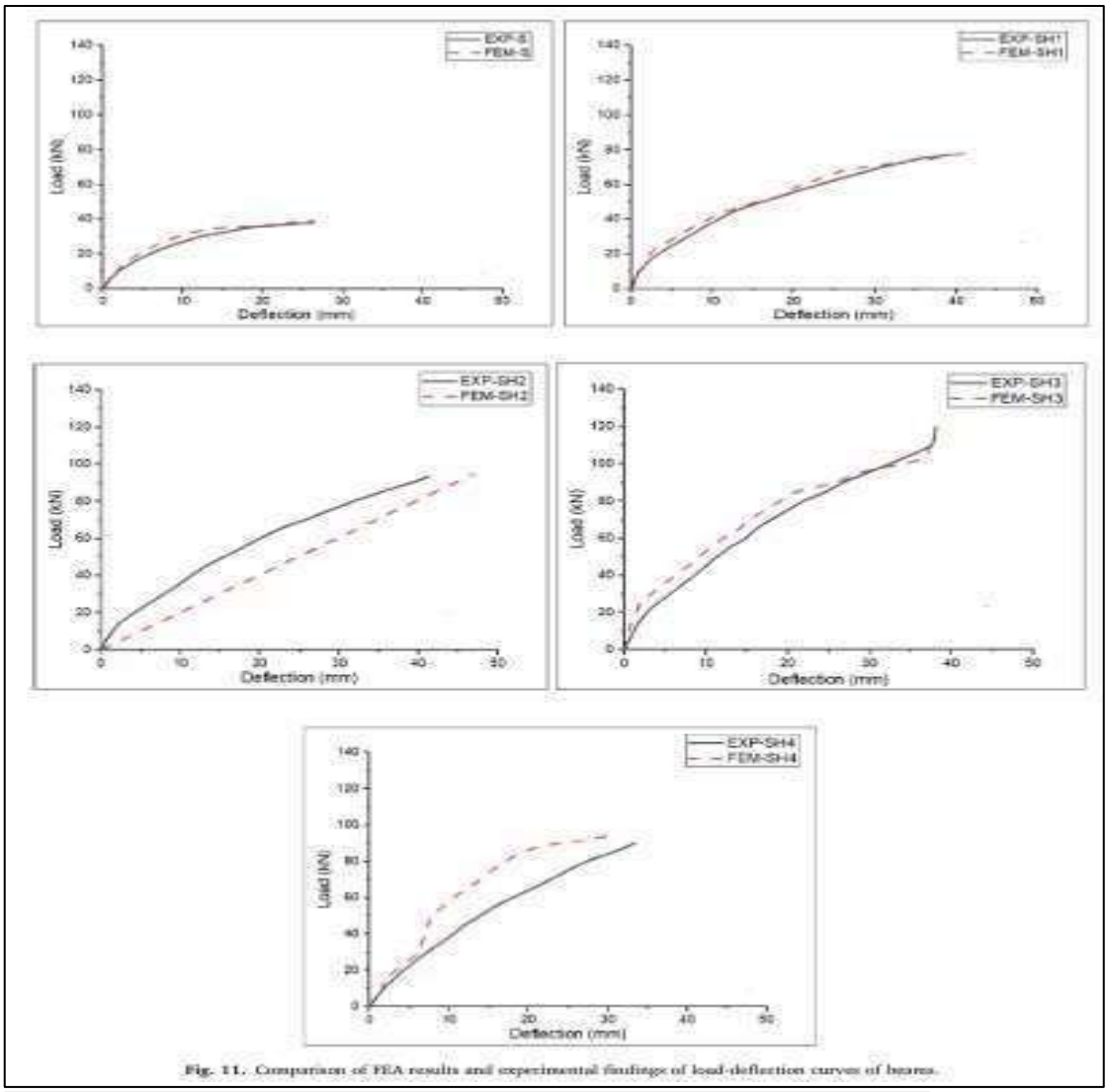


Fig. 11. Comparison of FEA results and experimental findings of load-deflection curves of beams.

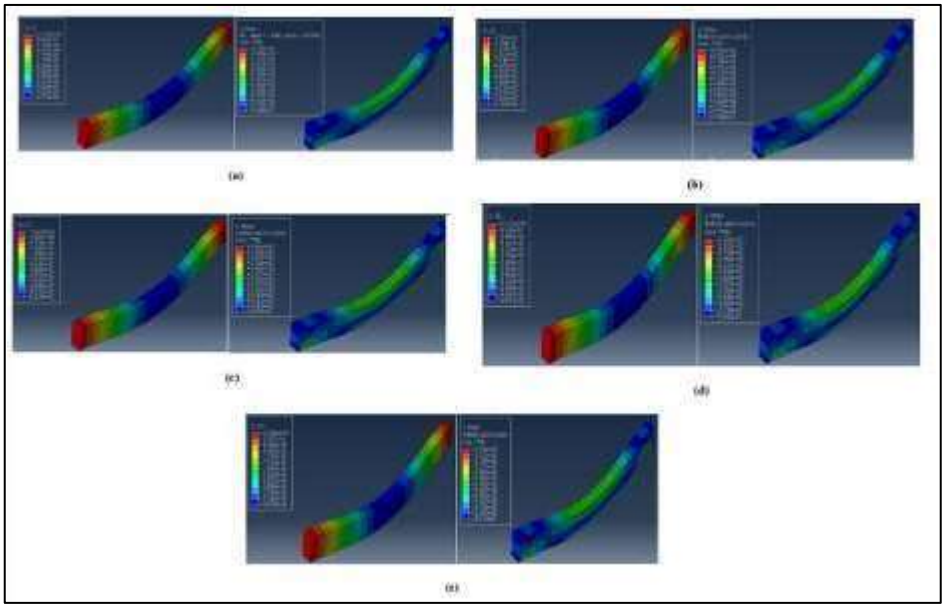

**Figure 12**

**Table 10 FE Simulation Results & Experimental Results**

| Specimen | % Difference Pu | % Difference δu | Experimental Pu (kN) | Experimental δu (mm) | Numerical δu (mm) | Numerical Pu (kN) |
|---|---|---|---|---|---|---|
| SH-5 | 2.67 | 0.69 | 38.00 | 26.23 | 26.41 | 39.04 |
| SH-1 | 1.28 | 4.29 | 77.00 | 39.24 | 41.00 | 78.00 |
| SH-2 | 2.07 | 12.19 | 93.00 | 41.27 | 47.00 | 94.97 |
| SH-3 | 6.50 | 2.49 | 115.00 | 38.03 | 39.00 | 123.00 |
| SH-4 | 5.26 | 6.40 | 90.00 | 33.44 | 31.43 | 95.00 |

**Table 11 RC Beam Deflection**

| Specimen | Service Load (kN) | δ_per (mm) | Permissible Deflection as per IS 456:2000 (mm) | δ_u / δ_per |
|---|---|---|---|---|
| S | 25.33 | 8.74 | 11.20 | 0.78 |
| SH1 | 51.33 | 19.33 | 11.20 | 1.73 |
| SH2 | 62.00 | 23.05 | 11.20 | 2.06 |
| SH3 | 76.67 | 22.30 | 11.20 | 1.99 |
| SH4 | 60.00 | 19.99 | 11.20 | 1.78 |

## **5.** DISCUSSION AND CONCLUSIONS

In this paper, experimental and numerical research on five reinforced concrete (RC) beams (one control beam and four beams reinforced with externally applied thicker layers of hybrid fiber-reinforced polymer (HFRP) laminates) are conducted to measure flexural behavior. These findings show that the flexural capacity of beam SH3 was the highest, with the maximum bending moment of 53.65 kN xm which is 202.63 percent of the weight on the control beam and 0.087 x 10-6 /m as the maximum curvature. The load-carrying capacity of the RC beams was greatly increased by increasing the thickness of the HFRP laminates, and the strength was increased up to 81 per cent at a laminate thickness of 5.6 mm, and this is where no further increase in flexural strength was realized. The FE model was in good agreement with the experimental data and especially with the load-deflection response, but ultimate load and deflection difference were noted to be 6.5 to 12.1. In general, the increase of flexural capacities in the strengthened beams (SH1-SH4) was significantly higher than in the control specimen, and the increase at the level of strength was 102.63, 144.74, 202.63 and 136.84, respectively. The strength beam energy absorption was also improved considerably, in both SH1, SH2 and SH3, with SH4 slightly low (2.80) in energy absorption than SH3. These results prove the sustainability of external HFRP laminate strengthening to enhance flexural strength and energy absorption of RC beams and point out the prospective of hybrid FRP composites as the promising method of flexural strengthening in the future.

**References**

3. Abbood, I. S., Odaa, S. A., Hasan, K. F., & Jasim, M. A. (2021). Properties evaluation of fiber reinforced polymers and their constituent materials used in structures - A review. *Materials Today: Proceedings*, *43*, 1003–1008. https://doi.org/10.1016/j.matpr.2020.07.636

4. Abdollahiparsa, H., Shahmirzaloo, A., Teuffel, P., & Blok, R. (2023). A review of recent developments in structural applications of natural fiber-Reinforced composites (NFRCs). *Composites and Advanced Materials*, *32*. https://doi.org/10.1177/26349833221147540

5. Altin Karataş, M., & Gökkaya, H. (2018). A review on machinability of carbon fiber reinforced polymer (CFRP) and glass fiber reinforced polymer (GFRP) composite materials. In *Defence Technology* (Vol. 14, Issue 4, pp. 318–326). China Ordnance Society. https://doi.org/10.1016/j.dt.2018.02.001

6. Chinnasamy, V., Subramani, S. P., Palaniappan, S. K., Mylsamy, B., & Aruchamy, K. (2020). Characterization on thermal properties of glass fiber and kevlar fiber with modified epoxy hybrid composites. *Journal of Materials Research and Technology*, *9*(3), 3158–3167. https://doi.org/10.1016/j.jmrt.2020.01.061

7. Derkowski, W., & Walczak, R. (2021). Possibilities of increasing effectiveness of rc structure strengthening with frp materials. *Materials*, *14*(6), 1–18. https://doi.org/10.3390/ma14061387

8. Diniţ˛ă, A., Ripeanu, R. G., Ilincă, C. N., Cursaru, D., Matei, D., Naim, R. I., Tănase, M., & Portoacă, A. I. (2024). Advancements in Fiber-Reinforced Polymer Composites: A Comprehensive Analysis. In *Polymers* (Vol. 16, Issue 1). Multidisciplinary Digital Publishing Institute (MDPI). https://doi.org/10.3390/polym16010002

9. Duvnjak, I., Klepo, I., Serdar, M., & Damjanović, D. (2021). Damage assessment of reinforced concrete elements due to corrosion effect using dynamic parameters: A review. *Buildings*, *11*(10). https://doi.org/10.3390/buildings11100425

10. Ghanem, H., Chahal, S., Khatib, J., & Elkordi, A. (2023). Experimental and Numerical Investigation of the Flexural Behavior of Mortar Beams Strengthened with Recycled Plastic Mesh. *Sustainability (Switzerland)*, *15*(7). https://doi.org/10.3390/su15075640

11. Kalyani, G., & Pannirselvam, N. (2023). Experimental and numerical investigations on RC beams flexurally strengthened utilizing hybrid FRP sheets. *Results in Engineering*, *19*. https://doi.org/10.1016/j.rineng.2023.101337

12. Lin, Q., Cao, P., Wen, G., Meng, J., Cao, R., & Zhao, Z. (2021). Crack coalescence in rock-like specimens with two dissimilar layers and pre-existing double parallel joints under uniaxial compression. *International Journal of Rock Mechanics and Mining Sciences*, *139*. https://doi.org/10.1016/j.ijrmms.2021.104621

13. mahboubizadeh, S., Sadeq, A., Arzaqi, Z., Ashkani, O., & Samadoghli, M. (2024). Advancements in fiber-reinforced polymer (FRP) composites: an extensive review. In *Discover Materials* (Vol. 4, Issue 1). Discover. https://doi.org/10.1007/s43939-024-00091-9

14. Ortiz, J. D., Khedmatgozar Dolati, S. S., Malla, P., Nanni, A., & Mehrabi, A. (2023). FRP-Reinforced/Strengthened Concrete: State-of-the-Art Review on Durability and Mechanical Effects. In *Materials* (Vol. 16, Issue 5). MDPI. https://doi.org/10.3390/ma16051990

15. Panahi, M., Zareei, S. A., & Izadi, A. (2021). Flexural strengthening of reinforced concrete beams through externally bonded FRP sheets and near surface mounted FRP bars. *Case Studies in Construction Materials*, *15*. https://doi.org/10.1016/j.cscm.2021.e00601

16. Qi, J., Ye, Y., Huang, Z., Lv, W., Zhou, W., Liu, F., & Wu, J. (2023). Experimental Study and Theoretical Analysis of Steel–Concrete Composite Box Girder Bending Moment–Curvature Restoring Force. *Sustainability (Switzerland)*, *15*(8). https://doi.org/10.3390/su15086585
17. Rincon, L. F., Moscoso, Y. M., Hamami, A. E. A., Matos, J. C., & Bastidas-Arteaga, E. (2024). Degradation Models and Maintenance Strategies for Reinforced Concrete Structures in Coastal Environments under Climate Change: A Review. In *Buildings* (Vol. 14, Issue 3). Multidisciplinary Digital Publishing Institute (MDPI). https://doi.org/10.3390/buildings14030562
18. Said, A., Elsayed, M., El-Azim, A. A., Althoey, F., & Tayeh, B. A. (2022). Using ultra-high performance fiber reinforced concrete in improvement shear strength of reinforced concrete beams. *Case Studies in Construction Materials*, *16*.
19. https://doi.org/10.1016/j.cscm.2022.e01009
20. Sbahieh, S., Mckay, G., & Al-Ghamdi, S. G. (2023). A comparative life cycle assessment of fiber-reinforced polymers as a sustainable reinforcement option in concrete beams. *Frontiers in Built Environment*, *9*. https://doi.org/10.3389/fbuil.2023.1194121
21. Shaheen, Y. B., Eltaly, B. A., Yousef, S. G., & Fayed, S. (2023). Structural Performance of Ferrocement Beams Incorporating Longitudinal Hole Filled with Lightweight Concrete. *International Journal of Concrete Structures and Materials*, *17*(1). https://doi.org/10.1186/s40069-023-00579-3
22. Sharba, A. A. K., Hussain, H. D., & Abdulhussain, M. (2021). Retrofitting of RC beams using FRP techniques: a review. *IOP Conference Series: Materials Science and Engineering*, *1090*(1), 012054. https://doi.org/10.1088/1757-899x/1090/1/012054
23. Siamakani, S. Y. M., Nagai, K., Jiradilok, P., & Sahamitmongkol, R. (2022). Prevention of concrete breakout failure of expansion anchor in tension by post-installed reinforcement: Discrete analysis and experiment. *Case Studies in Construction Materials*, *17*. https://doi.org/10.1016/j.cscm.2022.e01233
24. Smarzewski, P., Cao, M., Khan, M., Farooqi, M. U., Ostrowski, K. A., Chastre, C., Furtak, K., & Malazdrewicz, S. (2022a). *materials Consideration of Critical Parameters for Improving the Efficiency of Concrete Structures Reinforced with FRP*. https://doi.org/10.3390/ma
25. Smarzewski, P., Cao, M., Khan, M., Farooqi, M. U., Ostrowski, K. A., Chastre, C., Furtak, K., & Malazdrewicz, S. (2022b). *materials Consideration of Critical Parameters for Improving the Efficiency of Concrete Structures Reinforced with FRP*. https://doi.org/10.3390/ma